Review Of Research
Vol. 3, Issue. 3, Dec. 2013
Impact Factor 2.1002(UIF)
ISSN:-2249-894X Available online at www. lbp.world

ORIGINAL ARTICLE

SIZE MEASUREMENT OF METAL AND NANOPARTICLES VIA UV-Vis ABSORPTION SPECTRA

Sony Kumari
Research Scholar, Deptt. Of Physics, L.N.M.U, Darbhanga.

ABSTRACT :-

This paper reports for the novel and simple method for measurement of the size of metal and semiconductor nanoparticles. For metallic nanoparticles we selected Ag nanoparticles and synthesized these particles by laser ablation method. For size measurement of metal nanoparticles, Mie theory was used and found excellent agreement with image taken from TEM observation by experimental method. For semiconductor nanoparticles we chosen the cds nanoparticles and same way prepared by experimental method. For size measuremenbt, the effective mass model was used. Comparison between the result of theory and experiment has shown a good agreement for Cds nanoparticles.

KEYWORDS:-

Metal Nanoparticles, Semiconductor Nanoparticles, laser ablation method, size measurement, effective mass model.

INTRODUCTION

The preparation and study of Nano-size material is interest in research and technology because of in creasing their applications in electronic industry [1] and medical science [2] and partly because of increasing their unique character differing from the bulk state of those [3]. In the published reports have been proven the size and shape have an important role to brings unique properties for the nanopartilces [4].

Metal colloidal are one important nano-size material and laser ablation in solution is a new promising technique to obtain metal colloids [5]. One advantage of this method compared to other is producing pure colloids, which will be usefull for further applications. With using UV-vis absorption spectra we can characterize the nanoparticles prepared by laser ablation and survey their stability. By using Mie theory we are obtained a Lorentzian profile from uv-vis spectra of Ag nanoparticles and estimated the size of there nanoparticles between 4nm-8nm and also these results are compared with the size measurement obtained from TEM image.

We have applied the effective mass model for size measurement of Cds nanoparticles as a semiconductor. The quantum size effect in Cds nanoparticles was evidenced from the blue shifts of optical absorption edge and the average size of Cds nanoparticles was estimated by the magnitude of blue shift according to the effective mass model [6] .

Review Of Research
Vol. 3, Issue. 3, Dec. 2013
Impact Factor 2.1002(UIF)
ISSN:-2249-894X Available online at www. lbp.world

THEORETICAL APPROACHES

1. Metal nanoparticles

Mie theory based on the solid state which applies classical electrodynamics to cluster of simple shapes likes spheres. So we have assumed the resultant nanoparticles from ablation in distilled water to be spherical and widely spatially separated. The resulting Mie resonance casue selective optical extinction bands in the visible spectral range for the alkali and noble metals which usually depend strongly on the cluster diameter. For large size particles they are interpreted as spherical Plasmon polaritons, where as in small clusters they are referred to as collective electron excitations [7]. In following we summarized the predictions of the Mie theory for metal clusters that show cluster size effects in the optical spectra. This leads to theoretical models for the size dependencies of the dielectric functions and the definition of a relevant parameter which can be compared to experiment [8]. If particles are assumed to be spherical objects, widely dispersed (the average distance much larger than their radius) their cross section express as:

$$\sigma_{abs} = 9\frac{\omega}{c}\varepsilon_m^{3/2} v_0 \frac{\varepsilon_2(\omega)}{[\varepsilon_1(\omega)+2\varepsilon_m]^2+\varepsilon_2^2(\omega)} \quad (1)$$

Where v_0 is the spherical particles volume, ε_m and $\varepsilon_1(\omega) = \varepsilon_1(\omega) + i\,\varepsilon_2(\omega)$ denoted the dielectric function of the surrounding medium and particle material. The dipole resonance frequency is determined by the condition $\varepsilon_1(\omega) = 2\varepsilon_m$ provided. $\varepsilon_2(\omega)$ is not too large and dose not vary much near the resonance frequency. This cross section has a resonance peak whose position ω_1 is dependence on the dielectric functions. Within the Drude-Lorentz-Sommerfield free electron model [9] $\varepsilon(\omega)$ is given by

$$\varepsilon(\omega) = 1\,\frac{\omega_p^2}{\omega^2+i\omega\gamma} \quad (2)$$

Where the plasma frequency (ω_p) depends on the electron density (n) on the proper electron effective mass (m_{eff}). Using Eq. (2) and with new condition $\omega \approx \omega_1$. We can rewrite Eq. (1) in terms of a simple Loretzian, where the (FWHM) being given by the phenomenological damping constant γ.

$$\sigma_{abs} = \sigma_0 \frac{1}{[\omega-\omega_1]^2+\{\frac{\gamma}{2}\}^2} \quad (3)$$

With $\omega_1$being the Mie resonance frequency ($\omega_1 = \frac{\omega_p}{\sqrt{1+2\varepsilon m}}$). So the Drude γ of Eq. (2) equals the band width of the dipole Plasmon polariton in Eq. (3) for the case of free electron (only for the free electron metals) [10]. In the classical theory of free-electron metal, the damping is due to the scattering of the electrons with phonons, electrons, lattice defects, or impurities. The relation $\gamma = \frac{u_f}{L_\infty}$ holds where u_f is the Fermi velocity and $L_\infty$is the mean free path of the electron in bulk material [10]. If the cluster size becomes comparable with L_∞, the interaction of the conduction electrons with the particle surface becomes important as an additional collision process and increased γwhich depends on the closter size (expanded versions of Mie theory [7-8]).

$\gamma(R) = \gamma_0 + (Av_F)/R$ (4)

Where A attributed to scattering process (is $\frac{3}{4}$for silver [19]) and $\gamma_0$is the velocity of bulk scattering (for silver $5x10^{12}s^{-1}$) and v_f is the Fermi velocity (for silver $1.39x10^6$m/s) [12, 13]. Size depending of γ, leads to size depending of Polarizability), $\alpha(\omega, r)$or equivalently the dielectric function $\varepsilon(\omega, r)$ of the cluster material. When the size of particles is smaller than the average free path of the electrons (52nm for silver metal [11, 14]), the complex part of the silver dielectric function $\varepsilon(\omega) = \varepsilon_1(\omega)+i\,\varepsilon_2(\omega)$ modifies to

$$(\varepsilon_2 = \varepsilon_{2,bulk} + \frac{3\omega_p^2 v_f}{4\omega^3 r}) \qquad (5)$$

Here we have the angular frequency ω and the plasma frequency ω_p(for silver ω_p=1.380 x $10^{16}s^{-1}$ [2]). The mean free path limitation leads to an increased plasmon bandwidth with decreasing size of particle.

2. Semiconductor particles.

A number of theoretical models have been proposed in the literature, aiming to give a quantitative agreement of the predicted dependence of energy band gap on the crystal size (R) with the experimental data for a wide variety of semiconductor (with bulk band gap values within a wide rang). The most used theoretical model analysis of the experimental data for the energy band gap $E_g(R)$ dependencies is the Brus model (i.e. the effective mass approximation [12, 15]. According to the effective mass approximation model, the band gap of semiconductor nanoparticles (considered as a sphere with radius R) is given by:

$$E_g(R) = E_{g,bulk} + \frac{h^2}{8m_0R^2}\left(\frac{1}{m_e^*}+\frac{1}{m_h^*}\right) - \frac{1.8e^2}{\varepsilon_0\varepsilon_r R} - 0.248\frac{4\pi^2e^4m_0}{2(4\pi\varepsilon_0\varepsilon_R)^2h^2\left(\frac{1}{m_e^*}+\frac{1}{m_h^*}\right)} \quad .....(6)$$

Where $E_{e,bulk}$ is the bulk band gap value, h the plank's constant, m_0 the electron mass, while m^*_e and m^*_h are the electron and hole relative effective mass respectively, e the electron charge, $\varepsilon_0$the permittivity of vacuum and $\varepsilon_r$the relative dielectric constant of the semiconductor on the basis of Eq. (6) the band gap shipt with respect to the bulk value

$$\Delta E_g = \frac{h^2}{8m_0R^2}\left(\frac{1}{m_e^*}+\frac{1}{m_h^*}\right) - \frac{1.8e^2}{\varepsilon_0\varepsilon_r R} - 0.248\frac{4\pi^2e^4m_0}{2(4\pi\varepsilon_0\varepsilon_R)^2h^2\left(\frac{1}{m_e^*}+\frac{1}{m_h^*}\right)} \quad .....(7)$$

The first term in Eq. (7) referred to as the quantum localization term (i.e. the kinetic energy term), which shifts the E_g (R) to higher energies proportionally to R^{-2} . The second term in Eq. (7) arises due to the screened coulomb interaction between the electron and hole, it shifts the E_g (R) to lower energy as R^{-1}. The third, size-independent term in Eq. (7) is the salvation energy loss and is usally small and ignored [16].

Review Of Research
Vol. 3, Issue. 3, Dec. 2013
Impact Factor 2.1002(UIF)
ISSN:-2249-894X Available online at www. lbp.world

3. EXPERIMENTAL

Silver target 99.9%, 2mm thickness) first cleaned in detergent and then immersed in quartz cell with 20ml distilled water. The synthesis of silver nanoparticles were obtained by radiation of the ND:YAG laser. Laser radiation (532nm wavelength, 1Hz pulse repetition and 3mj pulse energy) was focused on the silver target by a local lens (F=50mm) through a liquid layer. The duration of the laser ablation experiment was 40mn. To make homogeneous distribution of the nanoparticles, the ablated solution was constantly stirred. After laser ablation experiement, the colloidal Ag nanoparticles were analyzed by UV-Vis spectrophotometer (Varian-Cary 100) in the range of 300nm to 800nm. Transmission electron microscopy (TEM: LEO-Model 912 AB) Measurements were performed by at 115 kVon Ag nanoparticles which were drop-costed onto a carbon-coated Au grid. For surveying the size changes of nanopartilces with the time, we measure UV-Vis absorption spectra in 10 days.

4. RESULTS AND DISCUSSION

Fig. 1 a shows the optical absorption spectra of colloidal solutions prepared at first day. The UV-Vis spectra reveal a characteristic absorption peak of the Ag colloidal located at 410 nm due to surface Plasmon resonance. On the basis of Mie theory and its expanded versions [7-8] information concerning Ag particle size can be derived from analysis of this spectrum. According to the Eq. (1), a Lorentzian fit (fig. 1b) of the absorption cross-section is expected with a resonance when the relationship $\varepsilon_1(\omega)$-$2\varepsilon_m$ is satisfied. The band width is strongly dependent on $\varepsilon_2(\omega R)$ and thus, on the particle size by Eq. (4) [10]. So with information presented metallic nanoparticles, we have been calculated the size of Ag nanoparticles 1.1 nm (at first day.)

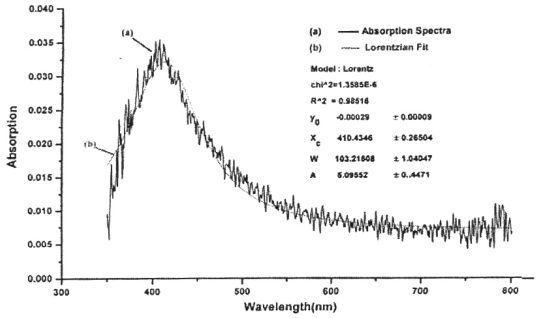

Fig. 1. (a) Optical absorption spectra of colloidal Ag nanopartilces prepared by laser ablation at first day. (b) Best fit of the optical surface Plasmon absorption spectra using Mie equation.

As seen colloidal solution was done for 10 days. After 10 days the maximum peak of absorption spectra is shifted up to 414 nm probably due to cluster density incensement. But width and intensity of the absorption spectra is broaden and smaller than located at 410 nm. A red shift of metallic particles (located at 414 nm) has been attributed to enlarge Ag particles.

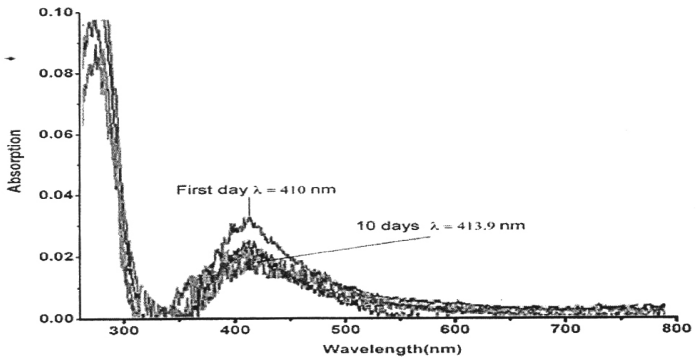

Fig. (2) Evaluation of colloidal Ag absorption spectra during 10 days.

Results of size measurements for Ag nanoparticles using Mie theory during 10 days listed in Table 1.

Table 2. Results of size measurements using Mie theory during 10 days.

Date	Position of peak	Width(nm)	Width(s^{-1})	Estimated size
First day	410 nm	108.21 nm	2.8×10^{14}	4.1 nm
Second day	411.91 nm	92.7 nm	2.6×10^{14}	4.4 nm
Third day	412.28 nm	75.1 nm	2.0×10^{14}	6.0 nm
Fourth day	413.8 nm	65 nm	1.6×10^{14}	7.9 nm
Tenth day	413.9 nm	60 nm	1.56×10^{14}	8.1 nm

As seen in Table 1. The width of the peak is decreased too from 108.21 nm to 60 nm after 10 days. It was shown previously, the surface Plasmon resonance is centered in the vicinity of 415 nm-425 nm which chemically technique was used to synthesis of Ag nanoparticles [17], whereas the absorption spectra of such structure prepared by laser ablation shown difference, in case the surface Plasmon resonance is shifted toward a short wavelength range between 400nm-415 nm due to influence of small-sized nanopartilces [18]. Our results confirmed this shift. The TEM image of Ag nanoparticles provided at first day in Fig. 3. has a good agreement with our estimation derived by Mie theory.

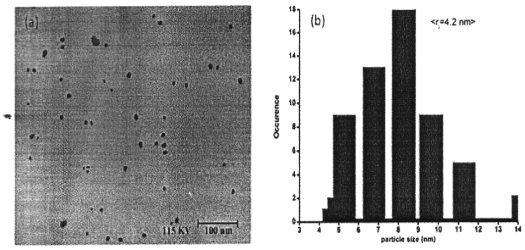

Fig. 3 (a) TEM image and (b) size distribution of colloidal Ag nanoparticles at first day. (<r>=4.2nm).

Different liquids such as THE, Acetone, Ethanol and Deionized water have been used to make different concentration of colloidal solution (Table 2.). Size measurement obtained from Mie theory by Loretzian fit and TEM image is compared in Table 2. From the presented results excellent agreement have found in the theory and experimental whereas the diversion theory and experiment is about 0.1 nm. For semiconductor measurements we selected Cds nanoparticles and estimated their size from UV-Vis absorption spectra with effective mass model because these semiconductors have a large band gap and good blue shift between bulk and nano-size. We measured the optical absorption edge of two Cds samples with different size 3.5 nm and 4nm, and calculated the magnitude of blue sift [19] with using the information of section 2.2. and Eq. 7. The results of this estimation and size measurement of these nanoparticles are in Fig. 4.

Liquid	Position of peak	Band width	Estimated size	TEM image
THF	411 nm	3.77×10^{14}	1.5 nm	1.6 nm
Acetone	400 nm	2.46×10^{14}	2.4 nm	2.5 nm
Ethanol	411 nm	0.8×10^{14}	10 nm	10.5 nm
Deionized water	405 nm	1.14×10^{14}	6 nm	6.5 nm

Table 2. Comparison the result of theory and experimental for size measurement of Ag nanoparticles.

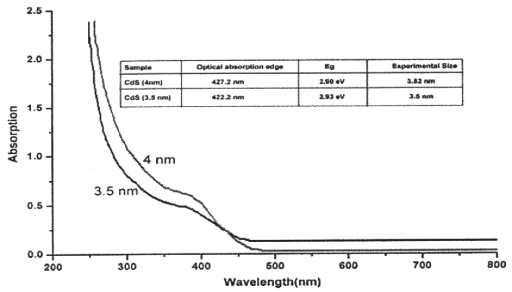

Fig. 4. UV-Vis absorption spectra and absorption edge measurement for two samples of Cds. (In set Table: Result of size measurement using UV- Vis absorption and effective mass model)

4.5. **DISCUSSION**

In this chapter we present a novel and simple method for measurement of the size of metal and semiconductor nanoparticles. For metallic nanoparticles we selected Ag nanoparticles and synthesized these particles by laser ablation method. For size measurement of metal nanoparticles, Mie theory was used and found excellent method. For semiconductor nanoparticles we was chosen the Cds nanopartilces and same way prepared by experimental method. For size measurement, the effective mass model was used. Comparison between the result of theory and experiment has shown a good agreement for Cds nanoparticles. With this method we can be measure, also, the energy band gap of semiconductor in a simply way.

REFERENCES

1. Lopez-Tocon, I.; Centeno, S.P; Otero, J.C; Marcos, J.I. Selection rules for the charge transfer enhancement mechanism in SERS: Dependence of the intensities of the L-matrix. J. Mol. Struct. 2001, 565-566, 369-372.
2. Lua, Z.; Fang, Y. Investigation of the mechanism of influence of colloidal gold/silver substrates in nonaqueous liquids on the surface.
3. Kundu, S.; Ghosh, S.K.; Pal, T. Photochemical deposition of SERS active silver nanopartilces on silica gel and their application as catalysts for the reduction of aromatic nitro compounds. J. Colloid Interface Sci. 2004, 272, 134-144.
4. Photopuulos, P.; Boukos, N.; Panogopouloum, M.; Meintains, N.; Pantiskos, N.; Raptis, Y.; Tsoukalas, D. Size control of Ag nanoparticles for SERS sensing applications. Procedia. Eng. 2011, 25, 280-283.
5. VIckova, B.; Pavel,; SLadkova, M.; Siskova, K.; Slouf, M. Single molecule SERS: Perpectives of analytical applications. J. Mole. Struct. 2007, 834-836, 42-47.
6. Kim, K.; Shin, D.; J.-Y.; Kim, K.L.; Shin, K.S. Suface-enhanced Raman scattering characteristics of 4-aminobenzenethiol derivatives adsorbed on silver. J. Phys. Che. C 2011, 115, 24960-24966.
7. A.D. McFarland, M.A. Young, J.A. Dieringer, R.P. Van Duyne, J. Phys. Chem. B, 109, 11279-11285, (2005).
8. M. Salerno, J.R. Krenn, B. Lamprecht, G. Schider, H. Diltbacher, N. Felidj, A. Leitner, F.R. Aussenegg, Opto Electronics Rev., 10, 217-224, (2002).
9. William L. Barnes, Nature Materials, 3, 588-589, (2004).
10. R.D. Averitt, D. Sarkar, N.J. Halas, Phys. Rev. Lett., 78, 4217-4220 (1997).
11. B.T. Drainer, P.J. Flatua, J. Opt. Soc. Am. A, 11, 1491-1499, (1994).
12. A Taflove, Computational Electrodynamics: The Finite Difference Time Domain Method, Boston, Artech House, 1995.
13. Ch. Hafner, Post modern electromagnetic using intelligent Maxwell solver, John-Wiley & Sons, 1999.
14. A Plaks, I. Tsukerman, G. Freidman, B. Yellen, IEEE Trans. On Magnetics, 39, 1436-1439, (2003).
15. C. Kittel, Introduction to Solid State Physics, Wiley, New York, 1976.
16. J. A.A. J. Perenboom, P. Wyder, F. Meier, Phys. Rev. B, 7, 173 (1981).
17. A.E. Neeves, M.H. Birnboim, J. Opt. Soc. Am. B., 6, 787-796, (1989).
18. P.B. Johnson, R.W. Christy, Phys. Rev. B., 6, 4370, (1972).
19. Ch. Hafner, J. Comp. Theo. Nanosci., 2, 88-98, (2005).
20. Nick N. Lepeshkin, Aron Schweinsberg, Giovanni Piredda et al., Phys. Rev. Lett., 93, 123902, (2004).

Review Of Research
Vol. 3, Issue. 3, Dec. 2013
Impact Factor 2.1002(UIF)
ISSN:-2249-894X Available online at www. lbp.world

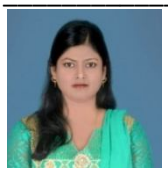

Sony Kumari
Research Scholar, Deptt. Of Physics, L.N.M.U, Darbhanga.